De Guzman, Joyce Ann T.; Markevich, Vladimir P.; Hawkins, Ian D.; Ayedh, Hussein M.; Coutinho, José; Binns, Jeff; Falster, Robert; Abrosimov, Nikolay V.; Crowe, Iain F.; Halsall, Matthew P.; Peaker, Anthony R.

Indium-Doped Silicon for Solar Cells—Light-Induced Degradation and Deep-Level Traps

Published in:
Physica Status Solidi (A) Applications and Materials Science

DOI:
10.1002/pssa.202100108

Published: 01/12/2021

Document Version
Publisher's PDF, also known as Version of record

physica status solidi a
www.pss-a.com

Indium-Doped Silicon for Solar Cells—Light-Induced Degradation and Deep-Level Traps

Joyce Ann T. De Guzman, Vladimir P. Markevich, Ian D. Hawkins, Hussein M. Ayedh, José Coutinho, Jeff Binns, Robert Falster, Nikolay V. Abrosimov, Iain F. Crowe, Matthew P. Halsall, and Anthony R. Peaker*

Indium-doped silicon is considered a possible p-type material for solar cells to avoid light-induced degradation (LID), which occurs in cells made from boron-doped Czochralski (Cz) silicon. Herein, the defect reactions associated with indium-related LID are examined and a deep donor is detected, which is attributed to a negative-*U* defect believed to be In_sO_2. In the presence of minority carriers or above bandgap light, the deep donor transforms to a shallow acceptor. An analogous transformation in boron-doped material is related to the B_sO_2 defect that is a precursor of the center responsible for BO LID. The electronic properties of In_sO_2 are determined and compared to those of the B_sO_2 defect. Structures of the B_sO_2 and In_sO_2 defects in different charges states are found using first-principles modeling. The results of the modeling can explain both the similarities and the differences between the B_sO_2 and In_sO_2 properties.

1. Introduction

Indium-doped silicon has been proposed as a possible p-type material for solar cells to avoid light-induced degradation (LID) observed in boron-doped Czochralski (Cz) silicon. However, the literature contains conflicting reports of LID in indium-doped material.[1–8] The situation is complicated by the incomplete ionization of indium resulting from its high activation energy of about 160 meV for hole emission. The unionized indium fraction acts as a recombination path, which shows a temperature and concentration dependence that tracks the ionization. An analysis of this recombination together with a study of indium-related LID has been reported recently by Murphy et al.[6]

The segregation coefficient of indium in silicon is low (5×10^{-4} compared to 0.8 for boron), so to get better doping uniformity appropriate for PV manufacture several methodologies have been investigated,[7,9–11] but recently continuous Cz growth (CCz) has been favored.[7,9] However, some manufacturers combine boron and indium doping to reduce the variation in hole concentration along the ingot. This makes the interpretation of LID in such a material extremely difficult.

Schmidt and Bothe compared the minority carrier lifetime stability of Si:In slices under illumination with that for boron, gallium, and aluminum-doped silicon and only observed LID in Si:B.[1] The Si:In had a resistivity of 14.5 Ω cm and an oxygen content of $\approx 7 \times 10^{17}$ cm^{-3}.[12] Binns et al.[7] also observed no measurable change in minority carrier lifetime in CCz Si:In with a resistivity of 3.8 Ω cm and $[O_i]$ of $(6.0 \pm 0.4) \times 10^{17}$ cm^{-3} after outdoor light soaking with a total irradiance of ≈10 kWh m^{-2}. Parallel experiments with boron-doped materials showed a degradation of lifetime from 160 to

J. A. T. De Guzman, V. P. Markevich, I. D. Hawkins, I. F. Crowe, M. P. Halsall, A. R. Peaker
Photon Science Institute and Department of Electrical and Electronic Engineering
The University of Manchester
Manchester M13 9PL, UK
E-mail: joyceann.deguzman@manchester.ac.uk

H. M. Ayedh
Department of Electronics and Nanoengineering
Aalto University
Tietotie 3, FI-02150 Espoo, Finland

The ORCID identification number(s) for the author(s) of this article can be found under https://doi.org/10.1002/pssa.202100108.

DOI: 10.1002/pssa.202100108

J. Coutinho
I3N and Department of Physics
University of Aveiro
Campus Santiago, Aveiro 3810-193, Portugal

J. Binns
Semiconductor and Device Research
Nexcel Electronic Technology
Gresham 97030, OR, USA

R. Falster
4 Harrison's Lane, Woodstock OX20 1SS, UK

N. V. Abrosimov
Leibniz-Institut für Kristallzüchtung (IKZ)
Max-Born-Straße 2, 12489 Berlin, Germany

20 μs over the same period. Cho et al.[5] fabricated passivated emitter and rear cell (PERC) and Al–BSF cells from 3.6 and 6.4 Ω cm In-doped CCz material ($[O_i] = 6.5 \times 10^{17}\,cm^{-3}$) and compared their LID with that in cells made from boron-doped CCz 6.2 Ω cm slices with the same oxygen concentration. They observed a drop in the average efficiency of the B-doped cells from 20.2% to 19.8% after 0.8 sun light soaking for 48 h at 37 °C but no change in the Si:In-based cells. In a recent work, Balaji et al. did not detect any degradation of efficiency of PERC solar cells made from In-doped Cz-Si with resistivity of 2.6 Ω cm and $[O_i] = 6.5 \times 10^{17}\,cm^{-3}$ after light soaking (1.0 sun illumination at 25 °C for 85 h), whereas the PERC cells made from B-doped Si with resistivity in the range 1.5–3 Ω cm and $[O_i] = 1 \times 10^{18}\,cm^{-3}$ degraded by 0.8% after the same irradiance.[8]

In contrast, other researchers have reported LID in In-doped Si materials. Möller and Lauer have undertaken detailed studies of Si:In LID and compared the effect with those occurring in boron, gallium, and aluminum-doped silicon.[2–4] They have used Si:In materials with resistivities in the range 3.8–8.6 Ω cm and $[O_i]$ in the range 1.1×10^{16} (FZ) to $1.8 \times 10^{18}\,cm^{-3}$ (Cz). Carbon concentrations were not given. They have made optical absorption measurements to determine the concentration of boron present in Si:In and understand whether the degradation was due to contamination with boron. The detection limit of shallow acceptor concentration in silicon by low-temperature Fourier-transform infrared absorption measurements can be lower than $1 \times 10^{12}\,cm^{-3}$ in careful experiments;[13] however, the detection limit of $[B_s]$ in In-doped Si has not been discussed in previous studies.[2–4] It was just reported that the boron was not detectable in all the In-doped Si samples used. This result indicated that boron contamination was insignificant in relation to Möller and Lauer's indium LID studies. As in the case of boron LID, two distinct degradation regimes are observed, a fast process and a slow process, with LID time constants in In-doped slices slightly shorter than those for the boron case when normalized to doping concentration.[2] Further, it was found that in one of the In-doped Cz-Si samples, the fast LID was more significant compared to the degradation during the slow process, as the fast LID accounted for more than 90% of the total normalized density of recombination active defects created during light soaking. In contrast, the slow LID in the B-doped Si accounted for more than 95% of the total normalized defect density.[2] The overall result is that the concentration of recombination active defects created by light soaking is slightly (<1.5 times) lower in In-doped samples than in the boron case when normalized to oxygen and carrier concentrations, and the degradation occurs 1.5–2 times faster in In-doped Si for comparable oxygen and dopant concentrations.[2] It has been further observed that the ratios of normalized concentrations of recombination active defects created during the fast and slow LID processes are different in In-doped Cz-Si samples with different oxygen contents; however, no explanation of this phenomenon was proposed.[3] An annealing step at 200 °C for 10 min deactivates the detrimental light-soaking-induced defect in Si:In and the lifetime is fully recovered as in the case of Si:B.

Murphy et al.[6] measured a range of CCz Si:In that contained no significant concentrations of boron with $[O_i]$ in the range of 3.8×10^{17}–$9 \times 10^{17}\,cm^{-3}$ and $[C_s]$ from 6.9×10^{15} to $3 \times 10^{16}\,cm^{-3}$. They observed a very fast initial degradation using light soaking with 1 sun intensity, seeing a 30% reduction in lifetime during the first second of exposure.

The BO LID has been recently linked to structural transformations of a complex consisting of a substitutional boron atom and two oxygen atoms (B_sO_2).[14–16] It has been shown that the B_sO_2 complex is a center with negative-U properties. This center is responsible for minority carrier trapping effects and has been identified as a source of persistent photoconductivity in Cz-Si:B material. The position of the Fermi level determines whether the defect is a deep donor or in one of a few configurations that have shallow acceptor levels. A configuration coordinate diagram has been constructed and the electronic characteristics of the defect have been determined using an analysis of the temperature dependencies of rates of carrier emission and capture by the deep donor trap in Si samples with different hole concentrations.[14,15]

During prolonged injection of minority carriers, the B_sO_2 complex transforms to a configuration with a shallow acceptor level and enhanced recombination activity.[14,16,17] This transformation results in a reduction of the minority carrier lifetime in boron-doped Cz-Si; i.e., it causes the BO LID of silicon solar cells. [14,16,17]

The limited and controversial results on LID in In-doped Si crystals, which are briefly described previously, do not allow a complete explanation for the origin of the observed controversies and an understanding of the defect reactions occurring upon light soaking in Si:In. The authors of the studies in which the LID effects in In-doped Si were reported suggested that the lifetime degradation after light soaking is related to the charge carrier capture and emission by a complex consisting of substitutional In atom and an interstitial silicon atom (In_{Si}–Si_i).[2–4] They further argued that such a complex with a substitutional boron instead of In is responsible for the LID in B-doped Cz-Si crystals.[2–4] However, the so-called A_{Si}–Si_i model of BO LID is not well accepted by the scientific community as it is not consistent with some solid experimental results available in the literature on the behavior of Si self-interstitial atoms and their interaction with substitutional boron atoms.[18–22] It was clearly shown in pioneering works by Watkins and coworkers[19,20] that such an interaction resulted in the appearance of an interstitial boron atom (B_i), the electronic and dynamic properties of which were studied thoroughly by means of the electron spin resonance (ESR) and deep-level transient spectroscopy (DLTS) techniques. According to ab initio calculations, the ground state structure of B_i consists of a B atom close to a substitutional site and a Si self-interstitial nearby,[23] so the B_i defect can be called B_{Si}–Si_i. There is solid experimental evidence that the B_i atoms are not stable at temperatures exceeding 250 K in boron-doped silicon crystals, to which these atoms were introduced by irradiation with megaelectronvolt electrons at cryogenic temperatures.[18–23] The disappearance of the ESR, DLTS, and infrared absorption signals due to the B_i atom upon annealing of the electron-irradiated Si:B crystals at $T > 250$ K was found to be accompanied by the appearance of other signals that could be self-consistently explained by diffusion of the B_i atoms and their interactions with other impurities (oxygen, carbon, substitutional boron) in the lattice.[18–23] The diffusion of the B_i atoms and their interactions with other impurities in Si crystals were considered in many experimental and theoretical papers,[18–28]

the results of which are not discussed in detail in this work. It should be mentioned only that some results on the B_i interactions in Si are still debatable.[25] For our consideration, it is important to note that in moderately B-doped $\{[B_s] \approx 10^{16}\,cm^{-3}\}$ p-type Cz-Si crystals the annihilation rate of B_i was found to be above $1 \times 10^{-4}\,s^{-1}$ at $T \geq 273$ K.[19] Therefore, after a storage of such Cz-Si:B crystals for a few minutes at room temperature the concentration of the B_i (B_{Si}–Si_i) centers in them tends to approach a negligible value.

Furthermore, it should be mentioned that the first-order complexes of the silicon self-interstitial with the most abundant impurities in the Si lattice (C_{Si}–Si_i or C_i, B_{Si}–Si_i, O_i–Si_i) with well identified ESR, DLTS, and IR absorption signatures have been detected only in Si crystals irradiated with high-energy particles and never been observed in as-grown Si crystals. However, different relatively large Si self-interstitial-related aggregates have been observed in some of the silicon ingots after growth.[29,30] These experimental observations can be explained on the basis of the results of ab initio calculations. According to the calculations, the binding energy of two Si self-interstitials in the di-interstitial complex, I_2, is ≈1.3–1.5 eV,[31] which significantly exceeds the binding energy of the B_{Si}–Si_i defect, which is about 0.2–0.3 eV.[24] Further agglomeration of Si_i into the larger I_n clusters is even more energetically favorable.[32,33] Therefore, the available experimental and modeling results indicate that Si self-interstitial atoms tend to agglomerate into I_n clusters upon growth of Si ingots,[29,30,32,33] and the appearance of interstitial-related point defects, such as B_i and C_i, in as-grown Si crystals is unlikely.

These arguments are also relevant for the consideration of the In_{Si}–Si_i defect in In-doped Cz-Si crystals. Furthermore, it was argued that the impurity atoms with small atomic radius, such as carbon and boron, are more attractive for Si interstitial atoms than impurity atoms with larger atomic radius such as indium.[18] Therefore, it is expected that the binding energy of In_{Si}–Si_i is even smaller than that for the B_{Si}–Si_i center, so the probability of the existence of the In_{Si}–Si_i defect in as-grown In-doped Si crystals is extremely low.

Minority carrier traps with properties similar to those for the B_sO_2 complex have been recently detected in Cz-Si crystals doped with Al, Ga, and In impurities.[34] In this work, we examine the defect reactions associated with minority carrier traps and their possible relation to minority carrier lifetime degradation upon light soaking of In-doped Si crystals. We have used Si:In grown by a CCz method that has no intentional boron added. The absence of boron has been confirmed by capacitance–temperature measurements.

2. Experimental and Modeling Details

In this work, we have studied electrically active defects in monocrystalline silicon that was grown via a continuous Czochralski (CCz) technique and doped with indium impurity atoms during growth. Five solar-grade CCz-Si:In wafers with resistivity in the range 1–17.5 Ω cm were used. Some information about the properties of the wafers is given in **Table 1**.

For characterization of the recombination properties of the In-doped Si wafers, measurements of minority carrier lifetime were conducted on the wafers. The wafers were cleaned, then dipped in a diluted HF solution, and put in a bag in contact with iodine/ethanol solution. This procedure reduces the surface recombination velocity to a low value (down to 6.5 cm s^{-1} for n-type Si crystals with resistivity in the range 3–5 Ω cm according to Al-Amin et al.[35]) and in slices with no subsurface damage provides a true measure of the bulk lifetime.[35] The lifetime maps were recorded at room temperature with the use of the microwave-detected photoconductance decay technique using a SemiLab WT-2000PVN machine.[36] The excitation pulses were provided by an InGaAs laser. The wavelength of the pulses was 905 ± 10 nm, their duration was 200 ns, and the measurements were conducted with the laser power providing 1.2×10^{13} photons/pulse. To determine the average lifetime values over a slice, we use an embedded SemiLab calculation procedure, which gives equal weighting to each point.

For the investigation of electrically active defects in the In-doped wafers, Schottky barrier diodes (SBDs) were fabricated on samples cut from the wafers. Prior to the fabrication of diodes, all samples were cleaned using trichloroethylene, acetone, and methanol for 5 min at each step. To remove the saw-cutting damage, polishing was carried out followed by etching using a 1:7 ratio of hydrofluoric acid and nitric acid solution ($HF:HNO_3$). The SBDs on indium-doped CCz-Si samples were prepared by plasma sputtering of a titanium/aluminum stack through a shadow mask. Subsequently, gold was deposited at the back of the sample to serve as an Ohmic contact. The diode area for all Cz-Si:In samples is about 0.79 mm^2, with a recorded leakage current of 1 μA at 10 V reverse bias. We note that there

Table 1. Details of the samples used in the study. Oxygen concentration [O_i] in the wafers was measured by infrared absorption measurements at room temperature according to the ASTM F121-83 procedure. The concentration of uncompensated shallow acceptors (N_a^-) in as-grown wafers was determined from *C–V* measurements on Schottky diodes at 300 K.

Sample	Dopant	Growth method	Resistivity [Ω.cm] (from growers)	N_a^- at 300 K [cm^{-3}]	Interstitial oxygen [O_i] [10^{17}, cm^{-3}]	Average value of effective lifetime [μs]
In-1	Indium	CCz	17.5	6.5×10^{14}	≈6	442
In-2	Indium	CCz	10.6	1.7×10^{15}	≈6	410
In-3	Indium	CCz	4.6	4.5×10^{15}	≈5	149
In-4	Indium	CCz	Not supplied	1.8×10^{16}	≈4	40
In-5	Indium	CCz	Not supplied	2.5×10^{16}	≈3	30
B-1	Boron	Cz	10	1.2×10^{15}	9.5 ± 1	Not measured
B-2	Boron	Cz	3.0	4.0×10^{15}	7.5 ± 1	Not measured

are no significant boron concentrations ($[B_s] \leq 0.02\ [In_s]$ according to our estimation) in the In-doped samples as verified by the measurements of temperature dependencies of capacitance of reverse-biased diodes. Some of the In-doped samples were subjected to a heat treatment at 700 °C for 20 min in Ar ambient for removal of oxygen-related thermal double donors (TDDs),[37,38] which can exist in the as-grown wafers.

For comparison, we studied samples from electronic-grade boron-doped Si wafers grown using the Czochralski (Cz) technique. The B-doped Si samples used have a resistivity of 3 and 10 Ω cm. We used n^+–p–p^+ junctions for Cz-Si:B, which were formed by implantation and subsequent thermal activation of 60 keV phosphorus ions (front side) and 60 keV boron ions (back side). Table 1 summarizes the details of all the samples used in this study.

We conducted current–voltage (I–V) and capacitance–voltage (C–V) measurements to assess the quality of the fabricated diodes and to determine the concentration of uncompensated shallow acceptors as well as the width of the depletion regions. DLTS and Laplace DLTS were used to detect and characterize deep-level traps.[39,40]

Electronic structure calculations within hybrid density functional theory were done using the Vienna Ab-initio Simulation Package (VASP).[41] The electronic exchange-correlation interactions were taken into account using the range-separated functional proposed by Heyd, Scuseria, and Ernzerhof (referred to as the HSE06 functional).[42] The projector-augmented wave method was used to treat the core electrons[43] and the valence states were expanded in plane waves with a cutoff energy of 400 eV. The Kohn–Sham equations were solved self-consistently until the total energy between two consecutive steps differed by less than 10^{-7} eV.

InO_2 complexes were inserted in 216-atom and 512-atom supercells of Si with cubic shape, made by replication of 3 × 3 × 3 and 4 × 4 × 4 conventional cells. The calculated lattice constant of Si was $a_0 = 5.4318$ Å. Forces acting on atomic nuclei were found using the Hellmann–Feynman theorem within the generalized gradient approximation (GGA) to the exchange-correlation potential.[44] These were minimized with respect to the atomic coordinates until the maximum residual force was $\leq$0.01 eV Å^{-1}. For the calculation of forces and structural relaxation (GGA level), the band structure was sampled on a Γ-centered 2 × 2 × 2 **k**-point grid in the Brillouin zone. However, for total energy calculations (HSE06-level), the sampling was done at the Γ-point (see Ayedh et al.[45] for further details).

The formation energy of defects is obtained as a function of the Fermi energy (E_F) using the usual expression

$$E_f(q, R; E_F) = E_{def}(q, R) - \sum_i n_i\mu_i + q(E_v + E_F) \quad (1)$$

where R and q stand for a specific configuration and charge state, respectively. On the right-hand side of Equation (1), E_{def} is the energy of the defective supercell made of n_i atoms of species i with chemical potential μ_i. The last term of the equation represents the energy required to transfer q electrons from a defect bound state into the Fermi level, located at E_F above the valence band top (E_v). Chemical potentials of Si, In, and O were found from bulk Si, substitutional In, and interstitial oxygen in silicon, respectively. Finally, we note that E_{def} includes a charge correction, obtained according to the recipe of Freysoldt, Neugebauer, and Van de Walle.[46]

3. Experimental Results

We determined the ionized uncompensated dopant concentration, $N_a^- = N_{A(total)} - N_D^+$, (where $N_{A(total)}$ is the total concentration of acceptors with energy levels in the lower half of the bandgap and N_D^+ is the concentration of compensating donor centers) in the In-doped samples with the use of capacitance–voltage measurements at 300 K. It should be noted that the values obtained are close to the concentrations of majority charge carriers after full ionization of traps with shallow and deep levels in the lower part of the Si gap.[47] It is important to take into account that in the case of In-doped Si, the concentration values derived from the C–V measurements differ significantly from equilibrium hole concentration values at 300 K because of only partial ionization of In atoms at this temperature at equilibrium conditions.[6] We have also estimated concentrations of oxygen-related TDDs in some of the In-doped wafers from a comparison of the N_a^- values in the pairs of neighboring samples, one of which was subjected to a TDD removal heat treatment at 700 °C for 20 min in Ar ambient. **Figure 1** shows typical concentration-versus-depth profiles, $N_a^-(W)$, for two samples, an as-grown one and a heat-treated one, from the In-3 wafer. Both the profiles show a strong drop in N_a^- close to the surface. This is due to the hydrogen passivation of substitutional acceptor atoms.[48] Hydrogen was introduced into the subsurface regions of the samples upon chemical treatments associated with their processing. The $N_a^-(W)$ values in the deeper bulk regions are constant. The difference of the bulk $N_a^-(W)$ values in the as-grown and heat-treated samples does not exceed 1.1×10^{14} cm^{-3}. Taking

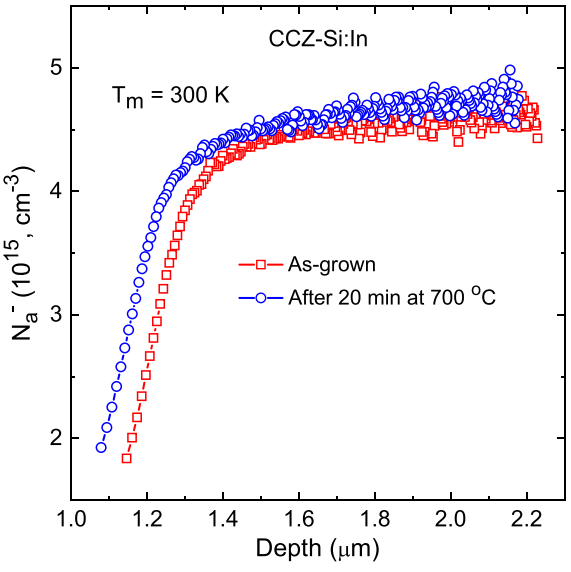

Figure 1. Depth profiles of the ionized uncompensated dopant concentration, $N_a^-(W)$, in as-grown and heat-treated (at 700 °C for 20 min) In-doped CCz-Si samples from the wafer denoted as In-3 in Table 1. The profiles have been calculated from the C–V dependences measured at 300 K.

into account the double-donor nature of the TDDs, concentration of these defects can be estimated as about $(5 \pm 1) \times 10^{13}$ cm^{-3} in our as-grown In-doped Si crystals. It should be noted that the acceptor concentration values given in Table 1 correspond to the bulk N_a^- values in the as-grown samples and we have studied recombination and electronic properties of In-related centers in these as-grown samples. In the analysis of the experimental results obtained, the measured bulk N_a^- values, which take into account the concentrations of TDDs and other compensating donor centers, have been used.

According to the results available in the literature, hydrogen is responsible for the so-called regeneration of BO-related recombination active defect upon illumination at elevated (100–200 °C) temperatures.[49–51] Further, it has been shown that the presence of hydrogen does not affect the kinetics of the BO-related degradation and dark annealing processes.[50,52] We monitored changes in the states of hydrogen in our In-doped samples by monitoring changes in the $N_a^-(W)$ dependencies after different treatments and measurements. However, as the "regeneration" and other effects of hydrogen were not the targets of this study, we designed our measurements for avoiding possible effects of hydrogen on the In- and B-related defects, which have been detected by DLTS. The majority of the DLTS measurements have been conducted by probing the bulk regions of the samples (e.g., the region from 1.6 to 2.2 μm in the samples, the $N_a^-(W)$ dependences of which are shown in Fig. 1), in which the hydrogen concentration was low.

Further, we have tried to obtain information about the ensemble of shallow-dopant impurities in the In-doped samples. For this purpose, measurements of temperature dependencies of bias capacitance, C_b, of the diodes were carried out. **Figure 2** compares $C_b(T)$ dependencies for the In-doped samples with the one recorded on a diode from B-doped Si. The sharp drops in the C_b values with decreasing temperature are related to the so-called carrier freezing, which depends on the activation energy of carrier emission from a shallow trap. It is clear that the temperatures of "carrier freezing" differ significantly in the In-doped samples and the B-doped one. The absence of capacitance in the region 50–100 K in indium-doped diodes is indicative that the silicon is intrinsic in this temperature range and confirms that there is no significant concentration of boron $\{[B_s] \leq 0.02\ [In_s]\}$ in the CCz-Si:In wafers, which have been studied.

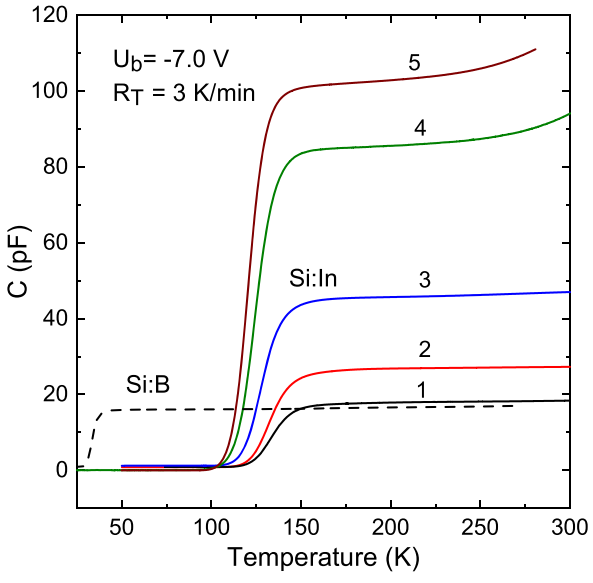

Figure 2. Capacitance of Schottky diodes at a bias voltage (U_b) as a function of temperature for the Si:In samples used in this work. A C(T) dependence for a Si:B sample is shown as a dotted line for comparison. The In-doped materials have carrier concentrations between (1) 6.5×10^{14} and (5) 2.5×10^{16} cm^{-3} at 300 K. The values of the bias voltage and the temperature rise rate (R_T) used for the C(T) measurements are given in the graph.

Lifetime maps were recorded on slices from the In-doped wafers and the average effective lifetime values are given in Table 1. In **Figure 3**, we have plotted the reciprocal values of the average effective lifetime in the as-grown In-doped samples versus the N_a^- concentration, which was determined from *C–V* measurements at 300 K. There is a clear correlation between the reciprocal lifetime and N_a^- values. The results obtained are consistent with the arguments presented in earlier studies that the un-ionized fraction of In, which increases with the increase in total In concentration, serves as an effective recombination center.[6]

Figure 4 shows LID associated with indium-doped silicon. The measurements were conducted at room temperature using a SemiLab WT-2000PVN with the excitation laser power providing 1.2×10^{13} photons/pulse. The slice was dipped in 2% HF and put in a bag in contact with iodine/ethanol solution. Although this procedure reduces the surface recombination velocity to a low values in slices with no subsurface damage, providing a true measure of the bulk lifetime,[35] in this case the slice was only etched (not chemo-mechanically polished) and some cutting damage remained, reducing the measured lifetime below the true bulk value. Despite this, it is evident that this material suffers from quite severe LID, particularly in the higher-lifetime regions at the slice center. The lifetime was fully recovered by

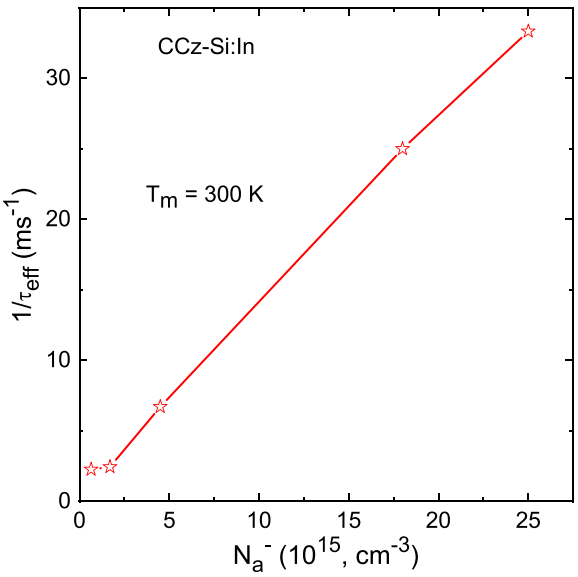

Figure 3. The reciprocal values of the average lifetime in the as-grown In-doped samples versus the N_a^- concentration, which was determined from C–V measurements at 300 K. The N_a^- and τ_{eff} values are given in Table 1.

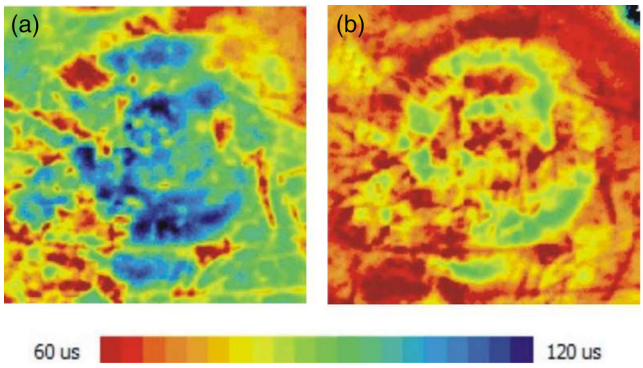

Figure 4. Lifetime maps of the central region (10×10 cm) of an 8 in. 0.72 mm thick Si:In 4.6 Ω cm wafer a) after 200 °C anneal for 30 min and b) the same area after exposure to 0.7 suns at 30 °C for 16.5 h.

annealing at 200 °C. The reason for the inhomogeneities is not known. Remeasuring the slice results in a very similar map, so it is assumed that the lifetime variations are not due to problems with the surface passivation process.

Figure 5 shows the DLTS spectra recorded in the temperature range from 300 to 420 K for the Schottky barrier diodes on indium-doped CCz silicon samples (Si:In-2 and Si:In-3) and n^+–p–p^+ diodes from boron-doped Cz silicon (Si:B). The magnitudes of the peaks are expressed in terms of the calculated trap concentration. It has been observed that the broad peak at 390 K that was detected in the B-doped Cz-Si as reported by Vaquiero-Contreras et al.[14] also occurs in the indium-doped samples with different hole concentrations. In the B-doped Si, this peak has been attributed to the double hole emission from the deep donor state of the complex containing a boron atom and an oxygen dimer referred as a boron-di-oxygen (B_sO_2) defect.[14,15] It has been found that depending on the position of the Fermi level in the silicon crystals, the B_sO_2 defect can either be a deep donor or a shallow acceptor.[14,15] In Cz-Si:B, this defect has been argued to be the precursor of the light-induced degradation (LID) defect, which is responsible for the reduction in the lifetime and efficiency of the silicon solar cells.[14,16,17]

It can be observed that the boron-doped Cz-Si and indium-doped samples (In-3) with almost similar doping concentrations of about (4.0–4.5) × 10^{15} cm^{-3} have a similar trap concentration in the range of (3.0–3.5) × 10^{13} cm^{-3}. It should be noted that the trap concentration values are derived using the equation: $N_T = 2(\Delta C/C_b) \times N_A \times f$, where f is the correction function.[39,53]

To further examine the electronic parameters of the defect, we have constructed Arrhenius plots of the hole emission rates for all the indium-doped CCz samples and plotted the values together with those for the boron-doped Cz-Si. As shown in **Figure 6**, the emission rates for all the samples are nearly equal. We have obtained identical values of activation energies (ΔE) of 0.97 ± 0.01 eV for both indium-doped CCz silicon and boron-doped Cz-Si. The pre-exponential factor values derived from the Arrhenius plots have also been found to be nearly the same in the range of (2.0 ± 1.0) × 10^8 $s^{-1}K^{-2}$ for all the samples.

We have also measured and analyzed the temperature dependencies of hole capture rates to determine the electronic characteristics of the detected trap in indium-doped CCz silicon samples. By means of Laplace DLTS, capture measurements were conducted in the temperature range 340–400 K. **Figure 7** shows changes in the hole population of the defect upon changes in filling pulse length measured at different temperatures in the range 360–390 K. It has been found that the hole capture process in all the studied samples can be described by a monoexponential equation, which allows an easy determination of characteristic

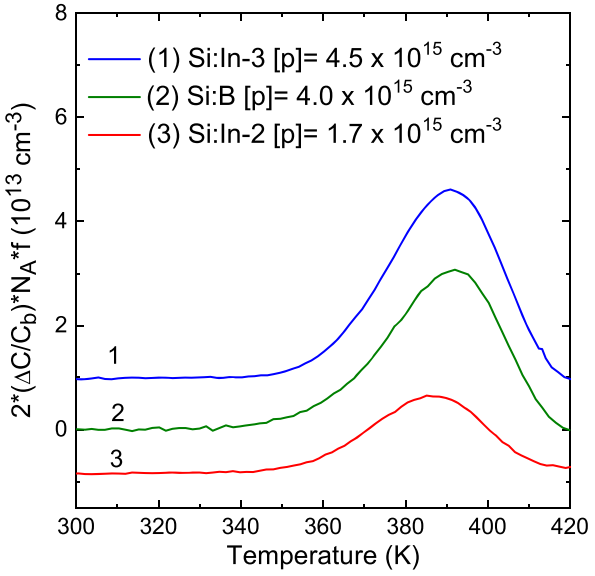

Figure 5. DLTS spectra recorded on as-manufactured Schottky diodes from CCz silicon material doped with indium impurity atoms and an n^+–p–p^+ diode from boron-doped Cz-Si. The emission rate window was 10 s^{-1} and filling pulse length was 200 ms. Spectra 1 and 3 are shifted on the vertical axis for clarity.

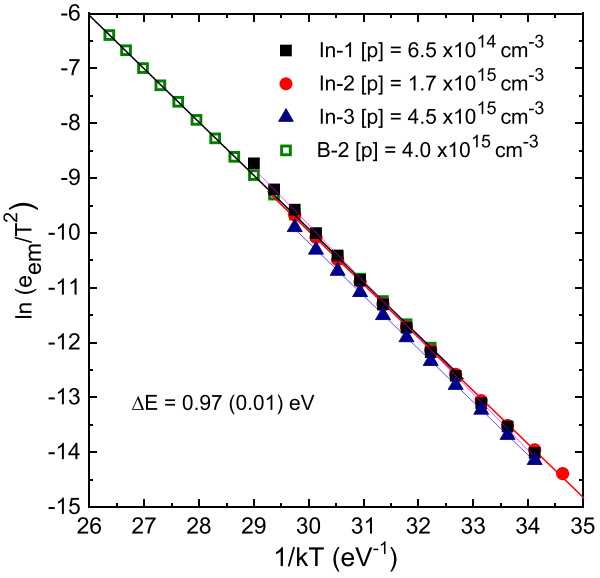

Figure 6. Arrhenius plots of hole emission rate measured in the temperature range 300–420 K on all Schottky and n^+–p–p^+ diodes from In-doped CCz-Si and B-doped Cz-Si, respectively. Laplace DLTS technique was used for the emission rate measurements. The calculated activation energy (ΔE) for all the samples is shown in the graph.

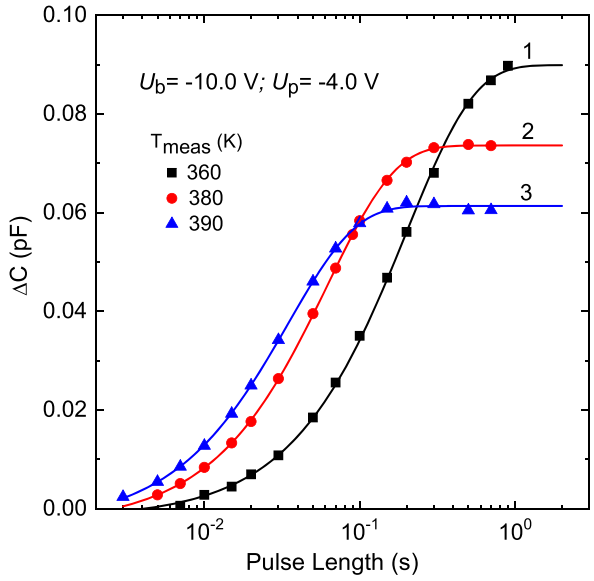

Figure 7. Capture kinetics of holes by the deep donor trap in a diode from the In-3 Si sample. Changes in magnitude of the capacitance transients, ΔC, due to hole emission from the deep donor trap upon changes in the filling pulse length are shown. The capacitance transients have been measured and analyzed with the use of the L-DLTS technique with the values of reverse bias voltage, U_b, and filling pulse voltage, U_p, given in the graph. The solid lines are calculated for a monoexponential growth process with least-squares fitting values of ΔC_{max} and characteristic growth rates.

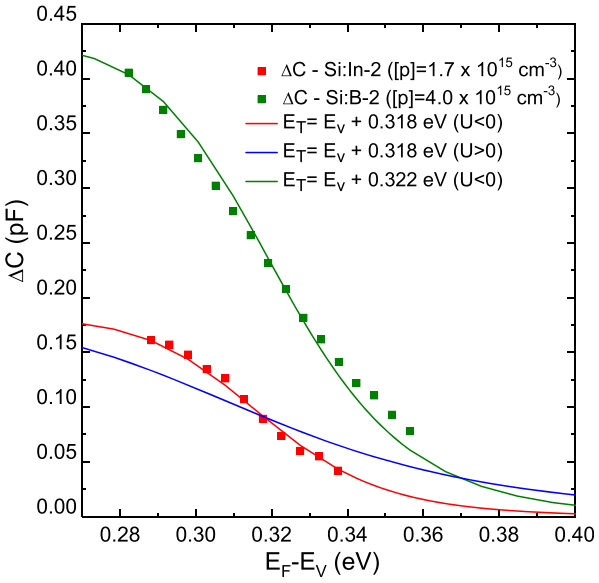

Figure 8. Occupancy level of the defect determined by capacitance measurements as a function of Fermi level position in the gap in In-doped CCz-Si and B-doped Cz-Si. The defect in the In-doped Si sample fits perfectly to the negative-U defect curve.

times of the capture process (τ_c) from fitting of the experimental data. It can be seen that the capture rate of holes is temperature-dependent, as is the maximum hole population of the center, which is directly proportional to the maximum achievable ΔC value, ΔC_{max}, at a given temperature. The change in ΔC_{max} value with temperature is the result of competition between capture and emission of holes in this temperature range. A brief consideration of temperature dependencies of the τ_c and ΔC_{max} values is further presented.

In recent studies by Vaqueiro-Contreras et al.[14] and Markevich et al.,[15] it has been reported that the B_sO_2 defect that is responsible for the hole emission signal with its maximum at 390 K in the DLTS spectra has negative-U properties.[54] Direct evidence of negative-U properties for a defect can be obtained from an analysis of temperature dependence of its occupancy ratio (occupancy function).[54] The occupancy function for a negative-U defect, $f_{U<0}$, differs from the Fermi function that describes the charge occupancy of defects with $U > 0$.[54] We investigated the occupancy function of the deep-level trap in indium-doped CCz-Si and found that the trap exhibits properties of a negative-U defect, similar to the B_sO_2 complex. **Figure 8** shows the changes in the ΔC_{max} values, which are directly proportional to the occupancy of defects with holes at a given temperature, against the position of the Fermi level relative to the valence band edge. The position of the Fermi level was determined using the equation $E_F - E_v = kT \ln(N_v/[p])$, where k is the Boltzmann constant, N_v is the effective density of states in the valence band, and $[p]$ is the concentration of holes. We found that the experimental $\Delta C_{max}(E_F)$ dependencies for both boron-doped Cz-Si and In-doped CCz-Si samples correspond to the occupancy function for a negative-U defect with the position of the occupancy level of the defect close to 0.32 eV above the valence band edge in both cases.

The results obtained indicate very similar hole emission and occupancy-level properties for the deep-level trap in B- and In-doped silicon. In the B-doped case, strong arguments have been presented that the trap is related to the B_sO_2 complex in Si:B.[14,15] Deep donor properties of the B_sO_2 defect are associated mainly with structural and electronic properties of the oxygen dimer. The results displayed in Figure 2 indicate a negligible concentration of boron atoms in the In-doped samples studied in our work. We suggest that the deep-level trap in In-doped samples could be associated with an In_sO_2 defect, with the oxygen dimer responsible for the donor properties of the center. This suggestion is supported by the results of ab initio modeling, which are shown subsequently. For deeper characterization of the shallow acceptor state of the defect in the In-doped Si samples, we analyzed temperature dependencies of transitions from the shallow-acceptor to deep-donor state (capture rates of holes).

Figure 9a shows the Arrhenius plots of the capture rates for three Schottky barrier diodes doped with indium impurity atoms. It appears that in the lower temperature range, the hole capture rate is faster in In-doped Si (In-3) samples with higher hole concentration, whereas in the higher temperature range, the capture process is faster by the In-sample (In-1) with the lowest concentration of holes. There are two slopes in all the $1/\tau$ ($1/kT$) dependencies, which indicate a change in the dominant mechanism of the hole capture process.[51] We have managed to describe all the experimental dependencies using equations for nonequilibrium occupancy statistics for defects with negative-U properties.[54,55] The solid curves in Figure 9 have been calculated according to Equation (47)–(49) from Coutinho et al.[54] with fitting

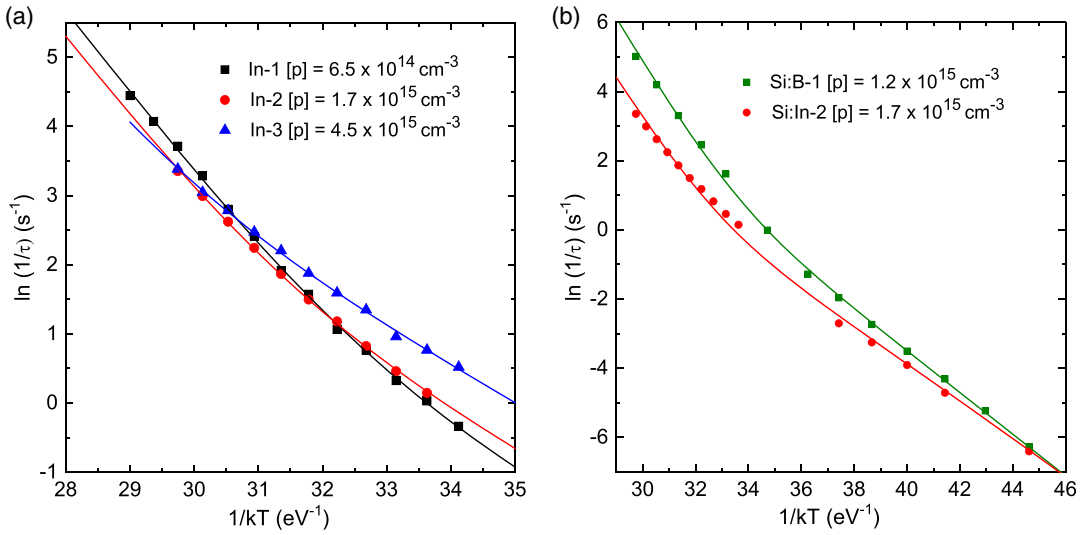

Figure 9. a) Temperature dependencies of capture rates of holes in the In-doped CCz-Si diodes and b) comparison of the capture rates between In-doped CCz-Si and B-doped Cz-Si with almost similar hole concentrations.

parameters for matching the experimental dependencies. The detailed analysis of the experimental $1/\tau$ $(1/kT)$ dependencies in the In-doped samples is beyond the scope of this work and will be reported in a separate study.

The capture data from In-doped samples were compared with those data recorded for the B_sO_2 defect in B-doped Cz-Si. It was found that for boron-doped Cz-Si and indium-doped CCz-Si with hole concentrations of 1.2×10^{15} and 1.7×10^{15} cm^{-3}, respectively, the hole capture rate of the In-doped CCz-Si materials is slower than the B_sO_2 defect, although the indium-doped silicon material has a slightly higher concentration of holes, as shown in Figure 9b. Further, we also investigated the capture rates for samples with higher concentration of holes in the range of $(4.0–4.5) \times 10^{15}$ cm^{-3} for both indium- and boron-doped samples. **Figure 10** shows a comparison of the capture kinetics measured at 290 K in Si:In and Si:B materials. Solid arguments have been presented earlier that in B-doped Si, this capture process is related to the transition from a shallow acceptor state to a deep donor state (hole capture) for the negative-U defects believed to be B_sO_2.[14,15] The decay rate is nearly three times slower in In-doped Si despite the slightly higher concentration of free holes in this material in comparison with the boron-doped Cz silicon. Based on the experimental data that we have obtained, we suggest that the transformation from shallow acceptor state to deep donor of the In_sO_2 complex in indium-doped silicon is relatively slower compared to the B_sO_2 complex in boron-doped Cz silicon. This could be one of the possible reasons for the reduced extent of LID in indium-doped silicon.

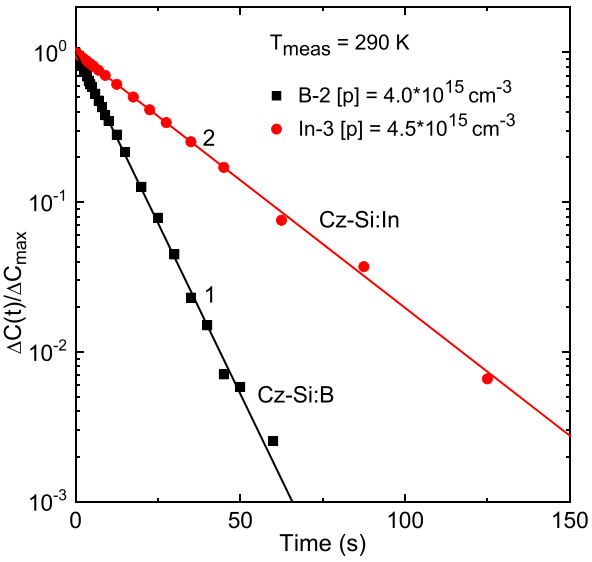

Figure 10. Normalized capacitance transient decays recorded at 290 K on the Schottky diodes from In-doped CCz silicon and n+–p–p$^+$ diodes from B-doped Cz silicon. Solid lines are calculated monoexponential decay with a decay rate value as a fitting parameter.

4. Modeling Results

The compliance of an In_sO_2 model, analogous to that of B_sO_2 from Vaqueiro-Contreras et al.,[14] with the observations reported earlier was verified by first-principles calculations. We investigated several complexes involving twofold and threefold coordinated oxygen atoms, essentially comprising two groups: D-form defects where the O_2 unit forms a ring structure, as shown in **Figure 11**a, and A-form defects where O_2 displays a staggered configuration (see Figure 11b). In the first group, In_sO_2 defects possess a donor transition close to the conduction band bottom, while in the second they are shallow acceptors. Further details regarding the electronic structure of these defects are given in Vaqueiro-Contreras et al.[14]

Figure 11a,b displays several Si ligands (white atoms) neighboring the oxygen dimer (red atoms). Each Si ligand was replaced by In, and the resulting configuration is hereafter referred to as

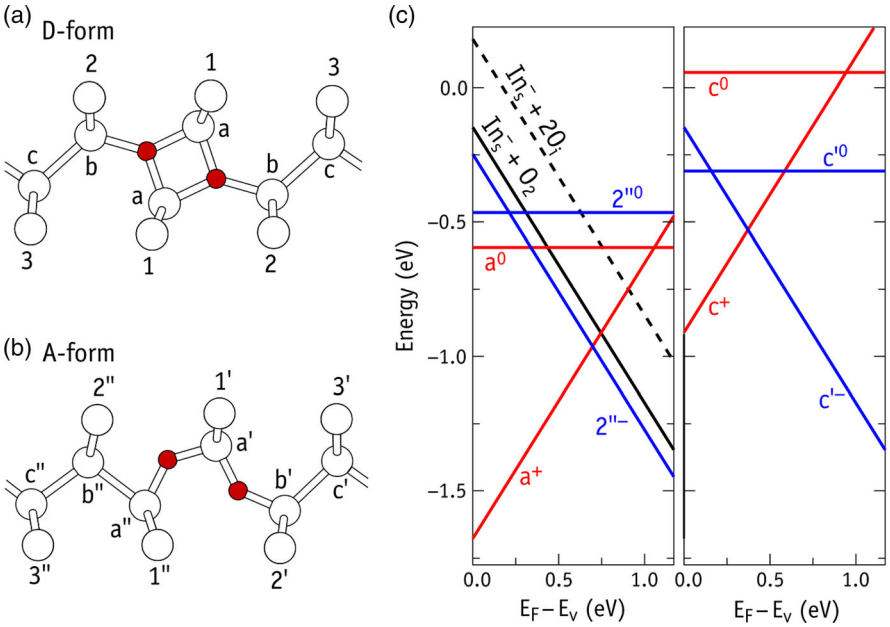

Figure 11. Atomistic models for In_sO_2 in silicon and respective formation energies. a) Donor state (D-form) and b) acceptor state (A-form). Oxygen and silicon are shown in red and white, respectively. In the donor and acceptor ground states, the indium atom replaces Si_a and $Si_{2''}$ atoms, respectively. c) Formation energy diagrams highlighting the negative-U character of the complex. Dashed and solid black lines represent energies of (uncorrelated) $In_s^- + 2O_i$ and $In_s^- + O_{2i}$ defects. Colored lines represent energies of In_sO_2 states (see corresponding labels).

In_sO_2 or simply X^q, with X and q corresponding to the site label and charge state, respectively. In p-type Si, positively charged D-form defects are the most stable. Configurations a^+, b^+, and c^+ show the lowest energies with respective binding energies $E_b = 1.5$, 1.3, and 0.7 eV for the reaction $In_s^- + O_2 + 2h^+ \rightarrow (In_sO_2)^+$. This involves the capture of two holes, whose energy was calculated from the valence band top eigenvalue of a bulk Si supercell. These figures compare with $E_b \approx 1$ eV for the most stable form of $(B_sO_2)^+$, and suggest a sizable driving force for the formation of In_sO_2 complexes in O-rich In-doped Si.

We note that for boron-di-oxygen, the ground state structure is $B_sO_2(1^+)$.[14] Here, apart from the hole capture and donor–acceptor Coulomb stabilization terms, the binding energy has a strain-relaxation contribution due to the opposite strain fields of boron and O_2. In the case of In_sO_2 the strain contribution is possibly repulsive due to the large size of the In atom. However, in a^+ and b^+ this effect is overridden by the strong oxidation energy of In, which establishes a direct bond with overcoordinated oxygen.

Among negatively charged A-form defects, only those with remote In substitutions, namely, 2″, 3′, and 3″, show positive binding energy for $In_s^- + O_2 \rightarrow (InO_2)^-$. For the first two structures $E_b = 0.1$ eV, while the latter is marginally bound ($E_b = 0.02$ eV). These configurations differ from that found for the stable $B_sO_2(1')$ counterpart.[14] Here, the analogous $In_sO_2(1'^-)$ state has a negative binding energy $E_b = -0.4$ eV due to superposition of compressive strain from both indium and O_2.

On the left-hand side of Figure 11c we show a formation energy diagram, constructed with the help of Equation (1), for defect states involving one substitutional In atom and two interstitial O atoms in silicon. The zero-energy refers to isolated neutral In and two O_i defects. The dashed line represents the formation energy of uncorrelated $In_s^- + 2O_i$ species. The solid black line represents uncorrelated In_s^- and the oxygen dimer ($In_s^- + O_2$). Its offset with respect to the dashed line is 0.33 eV, representing the binding energy of O_2.

The blue and red lines in Figure 11c stand for formation energies of A-forms and D-forms, respectively. About $E_b = 0.1$ eV below $In_s^- + O_2$, we find the formation energy of $In_sO_2(2''^-)$. The A-form 2″ structure has an acceptor transition calculated at $E_v + 0.22$ eV, which is slightly deeper than what is estimated for the In acceptor, i.e., $E_v + 0.18$ eV. The D-form (*a* structure) has a calculated (0/+) transition at $E_v + 1.08$ eV. Combining these, the calculations confirm that In_sO_2 is a negative-*U* defect with a (−/+) transition estimated at $E_v + 0.72$ eV.

The calculation of the aforementioned quantity considers the ground state configurations in the positive and negative charge states, a^+ and $2''^-$, which are quite distant in the configurational space. Hence, it is probably not comparable to the measured counterpart at about $E_v + 0.32$ eV (see Figure 8). If we assume that during hole emission/filling in the DLTS experiment 1) the O_2 unit shares the same crystalline plane with In and 2) O_2 does not have enough thermal energy to change its inhabiting plane, i.e., that O_2 motion is constrained to its inhabiting the [110]-Si chain, the most stable and accessible acceptor state from a^+, b^+, and c^+ is c'^-. The latter has an energy only 0.1 eV higher than $2''^-$. A formation energy diagram of these "in-plane" structures is shown on the right-hand side of Figure 11c. The (0/+) transition involving structure *c* is estimated at $E_v + 0.95$ eV, matching the measured hole emission energy of

0.97 eV for the hole trap in the In-doped samples. Considering the energies of the relevant structures, namely, c^+ and $c^{'-}$, we obtain a $(-/+)$ occupancy transition at $E_v + 0.38$ eV, in rather good agreement with the measurements.

5. Discussion

With the use of the DLTS and high-resolution Laplace DLTS techniques, we have observed a hole emission signal with $E_{em} = 0.97$ eV in CCz-grown indium-doped silicon samples. We have found that the electronic characteristics of the defect, which gives rise to this signal in indium-doped CCz-Si, are similar to the ones for an analogous defect detected in the diodes fabricated from Cz-Si doped with boron atoms. In boron-doped silicon, this hole emission signal has been associated with the deep donor state of the B_sO_2 defect, which in this state can be considered a minority carrier trap and is a precursor of the defect configuration that is responsible for the light-induced degradation of lifetime in boron-doped silicon cells.[14,15] It has been shown that the B_sO_2-related minority carrier trap transforms into a recombination active center upon prolonged injection of minority carriers either via forward biasing of the diodes or via illumination.[14,15]

Our experimental data have shown that a minority carrier trapping center is present in the CCz-grown silicon doped with indium atoms. Further, evidence has been found that the defect in indium-doped CCz-Si has negative-U properties similar to the B_sO_2 complex. We are certain that the defect we have detected in In-doped CCz-Si is not due to boron because our indium-doped CCz-Si samples were not intentionally doped with boron atoms. The absence of boron concentration is confirmed by our capacitance–temperature measurements.

It has been argued that the B_sO_2 defect is composed of a substitutional boron atom and two interstitial oxygen atoms, and the transformations of the oxygen dimer resulted in the transition of the defect from a deep-donor state to a shallow-acceptor state.[14,15] Based on our experimental results, as the hole emission rates and occupancy level position of the B_sO_2 defect are almost identical to those for the analogous defect in In-doped CCz-Si samples, it is most likely that the defect in Si:In is a combination of a substitutional indium atom and two oxygen atoms forming an In_sO_2 complex.

According to the modeling results, the In_sO_2 complex is most stable in the donor state adopting a square geometry (D-form state). This is due to the direct bond of substitutional In with O_2, which makes it more stable than the B_sO_2 complex. The D structure corresponds to the "annealed" state, an efficient electron trap, but the nonrecombination active form of the defect. Also, like B_sO_2, upon capture of electrons, the defect undergoes a transformation into a shallow-acceptor configuration, referred to as the A-form state. Although it is not clear which A-type structure corresponds to the recombination active defect, there are some differences with respect to B_sO_2, which should be explored in the future.

By examining the capture rates of the In_sO_2 defect, we found that the transition from A-state to D-state (backward reaction) is slower for the In_sO_2 defect than for the B_sO_2 complex, as shown in Figure 9b and 10. This finding indicates that the transition to a recombination-active state that is responsible for LID takes a longer time in In-doped CCz-Si compared to boron-doped Cz-Si. This could be due to the stable bond of In with the O_2 dimer in the D-state and the differences in the strain introduced by indium and boron to the silicon lattice. We would like to underline here that we have not yet undertaken an investigation of the behavior of the deep donor trap in the In-doped CCz-Si samples upon prolonged light soaking. This will be conducted in the near future to investigate a possible precursor–recombination center transition in indium-doped silicon. Therefore, at the moment our suggestion that the transformation of the In_sO_2 defect into the recombination active form upon light soaking is responsible for the LID effect in In-doped Cz-Si lacks a solid experimental confirmation.

Based on the ab initio calculations, the most stable acceptor states of the In_sO_2 defect can involve a large separation between In and O_2 units. Unlike in the $(In_sO_2)^+$ ground state, the In atom in the lowest-energy $(In_sO_2)^-$ state does not share the same crystalline plane as O_2, anticipating a large barrier for the minority-carrier-induced reaction $a^+ + e^- \rightarrow 2''^- + h^+$. The recombination active species could be one along the way of this conversion. A possible contender is $B_sO_2(c')$, where O_2 shares the same crystalline plane with the In atom. The complete or partially photoinduced transformation into the $2''^-$ ground state could depend on the thermal history of the silicon during growth and processing as well as the illumination and subsequent annealing during measurements. Such conditions could explain discrepancies in the literature regarding the observation of LID in In-doped cells.

6. Conclusion

Minority carrier traps were observed in CCz-grown silicon doped with indium atoms, which have similar electronic characteristics to those of the trapping centers detected in B-doped Cz-Si. This trapping center in boron-doped silicon solar cells is proposed to be the precursor of the defect responsible for light-induced degradation consisting of a substitutional boron atom and two oxygen atoms. Based on the experimental results and ab initio calculations, a minority carrier trap in indium-doped CCz silicon is suggested to be a complex composed of a substitutional indium atom and two oxygen atoms (In_sO_2). The calculations have shown that the In_sO_2 complex is more stable in its D-structure compared to B_sO_2, because the indium atom is directly bonded with two oxygen atoms, forming a square structure. We have conducted detailed measurements of hole emission and capture of the trap in In-doped CCz-grown silicon and observed that there is a significant difference in the transition rates from a shallow-acceptor state to the deep-donor state for In_sO_2 and B_sO_2. We have found that the A $\rightarrow$ D transition is significantly slower for the In_sO_2 complex compared to the B_sO_2 defect. This could be a possible reason for the discrepancies in the literature related to observations of LID in In-doped Cz-Si material.

Acknowledgements

The authors would like to thank EPSRC (UK) for funding this work via grant EP/TO25131/1. J.A.T.D.G. would like to thank the Government of the

Philippines through the Department of Science and Technology (DOST) for her Ph.D. funding. J.C. is thankful for the support of the i3N projects, Refs. UIDB/50025/2020 and UIDP/50025/2020, financed by the Fundação para a Ciência e a Tecnologia in Portugal.

Conflict of Interest

The authors declare no conflict of interest.

Data Availability Statement

The data that support the findings of this study are available from the corresponding author upon reasonable request.

Keywords

indium-doped silicon, light-induced degradation, oxygen recombination enhanced reactions, solar cells

Received: February 28, 2021
Revised: June 11, 2021
Published online:

[1] J. Schmidt, K. Bothe, *Phys. Rev. B* **2004**, *69*, 024107.
[2] C. Möller, K. Lauer, *Phys. Status Solidi RRL* **2013**, *7*, 461.
[3] C. Möller, K. Lauer, *Energy Proc.* **2014**, *55*, 559.
[4] K. Lauer, C. Möller, C. Teβmann, D. Schulze, N.V. Abrosimov, *Phys. Status Solidi C* **2017**, *14*, 1600033.
[5] E. Cho, Y. Ok, A. D. Upadhyaya, M. J. Binns, J. Appel, J. Guo, A. Rohatgi, *IEEE J. Photovoltaics* **2016**, *6*, 795.
[6] J. D. Murphy, A. I. Pointon, N. E. Grant, V. A. Shah, M. Myronov, V. V. Voronkov, R. J. Falster, *Prog. Photovolt. Res. Appl.* **2019**, *27*, 844.
[7] M. J. Binns, J. Appel, J. Guo, H. Hieslmair, J. Chen, T. N. Swaminathan, E. A. Good, in *Proc. 42th IEEE Photovoltaic Spec. Conf.*, IEEE, Piscataway, NJ **2015**, pp. 1–6.
[8] N. Balaji, V. Shanmugam, S. Raj, J. M. Y. Ali, M. L. O. Aguilar, I. J. Garcia, J. Rodriguez, A. Aberle, S. Duttagupta, *Sol. RRL* **2019**, *3*, 1900027.
[9] M. J. Binns, R. Scala, L. Bonanno, S. Haringer, A. Giannattasio, V. Moser (MEMC Electronic Materials) International Patent WO 2014/106086, **2014**.
[10] X. Yu, X. Zheng, K. Hoshikawa, D. Yang, *Jpn. J. Appl. Phys.* **2012**, *51*, 105501.
[11] S. Haringer, A. Giannattasio, H.C. Alt, R. Scala. *Jpn. J. Appl. Phys.* **2016**, *55*, 031305.
[12] Oxygen concentrations quoted in this paper have been determined according to the DIN 50 438/1 procedure, which is equivalent to "new" ASTM F 121-83.
[13] B. Pajot, *Optical Absorption of Impurities and Defects in Semiconducting Crystals. I. Hydrogen-like Centers. Vol. 158 of Springer Series in Solid-State Sciences*. Springer-Verlag, Berlin-Heidelberg, **2010**.
[14] M. Vaqueiro-Contreras, V. P. Markevich, J. Coutinho, P. Santos, I. F. Crowe, M. P. Halsall, I. Hawkins, S. B. Lastovskii, L. I. Murin, A. R. Peaker, *J. Appl. Phys.* **2019**, *125*, 185704.
[15] V. P. Markevich, M. Vaqueiro-Contreras, J. T. De Guzman, J. Coutinho, P. Santos, I. F. Crowe, M. P. Halsall, I. Hawkins, S. B. Lastovskii, L. I. Murin, A. R. Peaker, *Phys. Status Solidi A* **2019**, *216*, 1900315.
[16] J. A. T. De Guzman, V. P. Markevich, A. R. Peaker, M. Vaqueiro-Contreras, J. Coutinho, I. F. Crowe, I. Hawkins, S. Hammersley, M. P. Halsall, in *Proc. 37th Eur. Photovoltaics Sol. Energy Conf. Exhib.*, WIP, Munich, Germany **2020**, pp. 145–151.
[17] S. Jafari, Y. Zhu, F. Rougieux, J. A. T. De Guzman, V. P. Markevich, A. R. Peaker, Z. Hameiri, *ACS Appl. Mater. Interfaces* **2021**, *13*, 6140.
[18] G. D. Watkins, *Mater. Sci. Semicond. Proc.* **2000**, *3*, 227.
[19] a) G. D. Watkins, J. R. Troxell, *Phys. Rev. Lett.* **1980**, *44*, 593; b) J. R. Troxell, G. D. Watkins, *Phys. Rev. B* **1980**, *22*, 921.
[20] a) R. D. Harris, J. L. Newton, G.D. Watkins, *Phys. Rev. Lett.* **1982**, *48*, 1271; b) R. D. Harris, J. L. Newton, G.D. Watkins, *Phys. Rev. B* **1987**, *36*, 1094.
[21] R. D. Harris, G. D. Watkins, L. C. Kimerling, *Mater. Sci. Forum* **1986**, *10–12*, 163.
[22] L. C. Kimerling, M. T. Asom, J. L. Benton, P. J. Drevinsky, C. E. Caefer, *Mater. Sci. Forum* **1989**, *38–41*, 141.
[23] A. K. Tipping, R. C. Newman, *Semicond. Sci. Technol.* **1987**, *2*, 389.
[24] M. Hakala, M. J. Puska, R. M. Nieminen, *Phys. Rev. B* **2000**, *61*, 8155.
[25] L. Vines, E. V. Monakhov, A. Yu. Kuznetsov, R. Kozłowski, P. Kaminski, B. G. Svensson, *Phys. Rev. B* **2008**, *78*, 085205.
[26] O. V. Feklisova, N. A. Yarykin, J. Weber, *Semiconductors* **2013**, *47*, 228.
[27] L. F. Makarenko, B. S. Lastovskii, F. P. Korshunov, M. Moll, I. Pintilie, N. V. Abrosimov, *AIP Conf. Proc.* **2014**, *1583*, 123.
[28] L. F. Makarenko, B. S. Lastovskii, H. S. Yakushevich, M. Moll, I. Pintilie, *Phys. Status Solidi A* **2014**, *211*, 2558.
[29] S. Sadamitsu, S. Umeno, Y. Koike, M. Hourai, S. Sumita, T. Shigematsu, *Jpn. J. Appl. Phys.* **1993**, *32*, 3675.
[30] W. Von Ammon, E. Dornberger, in *Properties of Crystalline Silicon*, EMIS Datareviews Series No 20 (ed.: R. Hull) INSPEC, London, UK **1999**, Ch. 1.6.
[31] J. Kim, F. Kirchhoff, W. G. Aulbur, J. W. Wilkins, F. S. Khan, G. Kresse, *Phys. Rev. Lett.* **1999**, *83*, 1990.
[32] a) S. Lee, G. S. Hwang, *Phys. Rev. B* **2008**, *77*, 085210; b) S. Lee, G. S. Hwang, *Phys. Rev. B* **2008**, *77*, 085210; c) S. Lee, G. S. Hwang, *Phys. Rev. B* **2008**, *78*, 045204.
[33] L. A. Marqués, L. Pelaz, I. Santos, P. López, M. Aboy, *Phys. Rev. B* **2008**, *78*, 193201.
[34] J. A. T. De Guzman, V. P. Markevich, S. Hammersley, I. D. Hawkins, I. Crowe, N. V. Abrosimov, R. Falster, J. Binns, P. Alrermatt, M. P. Halsall, A. R. Peaker, in *Proc. 47th IEEE Photovoltaic Spec. Conf.*, IEEE, Piscataway, NJ **2020**, pp. 1013–1018.
[35] M. Al-Amin, N. E. Grant, A. I. Pointon, J. D. Murphy, *Phys. Status Solidi A* **2019**, *216*, 1900257.
[36] https://semilab.com/category/products/minority-carrier-diffusion-length-measurement
[37] P. Wagner, J. Hage, *Appl. Phys. A* **1989**, *49*, 123.
[38] C. A. J. Ammerlaan, in *Properties of Crystalline Silicon, EMIS Datareviews Series No 20* (ed.: R. Hull), INSPEC, London, UK **1999**, Ch. 11.4.
[39] A. R. Peaker, V. P. Markevich, J. Coutinho, *J. Appl. Phys.* **2018**, *123*, 161559.
[40] L. Dobaczewski, A. R. Peaker, K. Bonde Nielsen, *J. Appl. Phys.* **2004**, *96*, 4689.
[41] G. Kresse, J. Furthmüller, *Comput. Mater. Sci.* **1996**, *6*, 15.
[42] a) J. Heyd, G.E Scuseria, M. Ernzerhof, *J. Chem. Phys.* **2003**, *118*, 8207; b) Erratum in *J. Chem. Phys.* **2006**, *124*, 219906.
[43] P.E. Blöchl, *Phys. Rev. B* **1994**, *50*, 17953.
[44] J.P Perdew, K. Burke, M. Ernzerhof, *Phys. Rev. Lett.* **1996**, *77*, 3865.
[45] H. M. Ayedh, E. V. Monakhov, J. Coutinho, *Phys. Rev. Materials* **2020**, *4*, 064601.
[46] C. Freysoldt, J. Neugebauer, C.G. Van de Walle, *Phys. Rev. Lett.* **2009**, *102*, 016402.

[47] A. R. Peaker, V. P. Markevich, in *Defects and Impurities in Silicon Materials, Lecture Notes in Physics 916* (Eds.: Y. Yoshida, G. Langouche) Springer, Japan **2015**, Chapter 3.
[48] A. R. Peaker, V. P. Markevich, L. Dobaczewski, in *Defects in Microelectronic Materials and Devices* (Eds.: D. M. Fleetwood, S. T. Pantelides, R. D. Schrimpf) CRC Pres, Boca Raton, FL **2009**, Chapter 2.
[49] A. Herguth, G. Schubert, M. Kaes, G. Hahn, *Progr. Photovolt.: Res. Appl.* **2008**, *16*, 135.
[50] A. Herguth, B. Hallam, *AIP Conf. Proc.* **2018**, *1999*, 130006.
[51] B. Hallam, A. Herguth, P. Hamer, N. Nampalli, S. Wilking, M. Abbott, S. Wenham, G. Hahn, *Appl. Sci.* **2018**, *8*, 10.
[52] N. Nampalli, H. Li, M. Kim, B. Stefani, S. Wenham, B. Hallam, *Sol. En. Mat. Sol. Cells* **2017**, *173*, 12.
[53] D. Stievenard, D. Vuillaume. *J. Appl. Phys.* **1986**, *60*, 973.
[54] J. Coutinho, V. P. Markevich, A. R. Peaker, *J. Phys.: Condens. Matter* **2020**, *32*, 323001.
[55] V. P. Markevich, L. I. Murin, T. Sekiguchi, M. Suezawa, *Mater. Sci. Forum* **1997**, *258–263*, 217.